Chemical Visualization of Phosphoproteomes on Membrane*[S]

Anton Iliuk, X. Shawn Liu, Liang Xue, Xiaoqi Liu, and W. Andy Tao‡

With new discoveries of important roles of phosphorylation on a daily basis, phospho-specific antibodies, as the primary tool for on-membrane detection of phosphoproteins, face enormous challenges. To address an urgent need for convenient and reliable analysis of phosphorylation events, we report a novel strategy for sensitive phosphorylation analysis in the Western blotting format. The chemical reagent, which we termed pIMAGO, is based on a multifunctionalized soluble nanopolymer and is capable of selectively binding to phosphorylated residues independent of amino acid microenvironment, thus offering great promise as a universal tool in biological analyses where the site of phosphorylation is not known or its specific antibody is not available. The specificity and sensitivity of the approach was first examined using a mixture of standard proteins. The method was then applied to monitor phosphorylation changes in *in vitro* kinase and phosphatase assays. Finally, to demonstrate the unique ability of pIMAGO to measure endogenous phosphorylation, we used it to visualize and determine the differences in phosphorylated proteins that interact with wild-type and kinase dead mutant of Polo-like kinase 1 during mitosis, the results of which were further confirmed by a quantitative phosphoproteomics experiment. *Molecular & Cellular Proteomics 11: 10.1074/mcp.O112.018010, 629–639, 2012.*

Protein phosphorylation is an essential post-translational modification that regulates numerous cellular functions, including cell cycle progression, proliferation, differentiation, signal transduction, and apoptosis (1). It is arguably the most common covalent modification of proteins, and irregularities in phosphorylation network are a major cause of onset and progression of many diseases, most notably cancer (2). Consequently, detection of protein phosphorylation is essential in further understanding of the signaling pathways of an organism to prevent and treat such abnormalities.

Antibody-based detection on membrane, *i.e.*, Western blotting, has remained as the most basic biochemical method for the analysis of proteins, including phosphorylated proteins. In a typical Western blotting procedure, where proteins are separated on a gel, transferred onto a membrane, and detected by chemiluminescence or the like, a phospho-specific antibody is usually required to visualize specific phosphoproteins. There are general phospho-specific antibodies available, but at present, only anti-phosphotyrosine antibodies are of the required specificity (3). Phosphoserine and phosphothreonine residue detection is still sequence-dependent, resulting in partiality of these antibodies. Most research groups currently use phosphosite-specific antibodies developed for their protein of interest. However, prior knowledge of specific phosphorylation sites is required, thus limiting the analysis to only well characterized phosphorylation events. Phospho-specific antibodies typically cost much more to generate, whereas the quality often is difficult to control compared with a general antibody.

Another commonly used technique for phosphoprotein detection is radioactive labeling with ^{32}P (4). In addition to working with dangerous radioactive material, a major disadvantage of this approach is the difficulty of identifying physiological phosphorylation. This arises from the toxic effects ^{32}P has on cells, inducing DNA fragmentation, changing cell morphology, causing cell cycle arrest, and eventually resulting in apoptosis (5, 6). As a result, radioactive analyses of protein phosphorylation are more commonly carried out *in vitro*.

Mass spectrometry has emerged as a powerful tool to analyze protein modifications, including the identification of phosphorylation sites (7, 8), but many challenges remain mainly because of low ionization efficiency and poor fragmentation of phosphopeptides (9). Furthermore, many groups do not have access to such an instrument on daily basis because of high cost and technical requirements to operate the instrument. Phosphorylation analysis by mass spectrometry typically requires high resolution and high mass accuracy. Few bench-type instruments, therefore, are available for phosphorylation analysis, limiting it as a routine analytical technique in a typical biology laboratory.

Development of a staining/blotting method that selectively detects only phosphorylated proteins without the prejudice of amino acid microenvironment would therefore be of high value. There have been a number of attempts to introduce such a reagent that could specifically and sensitively bind to a phosphate group for visualization. One of the first developments was "Stains-All," a cationic dye that could bind to phosphorylated proteins in a gel. Unfortunately, its poor sen-

From the Department of Biochemistry and Purdue Center for Cancer Research, Purdue University, West Lafayette, Indiana 47907

Received February 12, 2012, and in revised form, May 10, 2012
Published, MCP Papers in Press, May 16, 2012, DOI 10.1074/mcp.O112.018010

sitivity and a high affinity for DNA, RNA, and acidic proteins greatly limited its applications (10, 11). Pro-Q Diamond is another phosphoprotein-specific stain developed by Molecular Probes, which had an improved selectivity compared with "Stains-All" (12, 13). Pro-Q dye is based on fluorescent signal detection and has been successfully used by some groups for the in-gel staining, particularly for two-dimensional gels (14–16). Although there were attempts to utilize it on a PVDF or nitrocellulose membrane (17), some background fluorescence of the nonspecific binding of the reagent and the lower selectivity of the Pro-Q Diamond stain make it difficult to confidently identify phosphoproteins after transfer. As a result, Pro-Q Diamond has most commonly been used for in-gel phosphoprotein detection. A different staining method termed Phos-tag employs dinuclear Zn^{2+} metal ion complex (18) for phosphoprotein detection. Combined with a chemiluminescence-based detection system, the technique was introduced to an application on PVDF membranes, enabling Western blot-like detection of the phosphoproteins. Although the Phos-tag reagent has been employed to detect phospho-containing species (18), the background and non-phospho-specific signals still remain high (19). Because of these drawbacks, the reagent, therefore, has been primarily used to identify phosphorylation by a gel shift or to detect isomers of multiphosphorylated proteins by incorporating the reagent during the preparation of SDS-PAGE gels (20, 21).

Titanium ion (IV) and TiO_2 have been demonstrated to possess superior selectivity toward phosphorylated residues on numerous occasions, particularly when selectivity "enhancers" are used (22–24). In our lab, we have demonstrated the unparalleled utility of titanium-based enrichment under homogeneous conditions. We have previously functionalized soluble nanopolymer (dendrimer) with multivalent Ti(IV) ions (termed PolyMAC) for phosphopeptide enrichment prior to mass spectrometry analysis, exhibiting extraordinary high selectivity, sensitivity, and reproducibility (25). Recently, we have also adopted the successful concept of titanium-functionalized nanopolymer to phosphoprotein detection in ELISA format, which we termed pIMAGO (phosphorimaging)[1] (26). We have demonstrated the great utility of the pIMAGO reagent for selective detection of phosphoproteins directly immobilized on a 96-well plate.

Here, we have applied the same concept for the detection of phosphoproteins using one of the most common biochemical techniques, Western blotting. Each pIMAGO molecule is synthesized to contain multiple titanium metal ions for selective binding to phosphates and multiple biotin groups for sensitive detection. After incubation with a membrane where phosphoproteins are bound, the reagent can be detected by chemiluminescence with horseradish peroxidase (HRP) conjugated to avidin or by fluorescence. Under acidic conditions, the reagent is capable of specifically binding only to phosphorylated sites without any bias toward amino acid sequences. Another feature of the pIMAGO reagent is the high ratio of biotin groups per reagent, resulting in significant enhancement and amplification of the signal; thus, even a protein with a low phosphorylation level can be detected. Without the usage of radioisotopes or expensive phospho-specific antibodies, the technique is capable of detecting protein of interest phosphorylated under physiological conditions, in the format of a standard Western blotting procedure. Alternatively, the reagent can be functionalized with fluorescent molecules instead of biotin to enable direct fluorescence-based detection.

Overall, the new approach displays superior selectivity toward phosphorylated proteins, enhanced sensitivity and lower cost compared with available commercial reagents. Here, we demonstrate the utility of pIMAGO to detect phosphorylated proteins in simple and complex protein mixtures, as well as during *in vitro* kinase and phosphatase assays. We have further shown that the technique is sensitive and specific enough to detect endogenous phosphorylation changes by analyzing Polo-like kinase 1 (Plk1) and its mutant protein complexes isolated directly from cells. The results were validated by quantitative mass spectrometry analysis, confirming a number of known Plk1 substrates and interacting proteins and identifying several new potential targets.

EXPERIMENTAL PROCEDURES

Materials—All of the reagents for pIMAGO synthesis, protein dephosphorylation, kinase assays, cell lysis reagents, trypsin, IP reagents, anti-FLAG antibodies and beads, and all standard proteins were obtained from Sigma-Aldrich. Anti-Thr(P) antibody was purchased from Cell Signaling Technologies. SnakeSkin dialysis tube and SuperBlock T20 blocking buffer were bought from Thermo Pierce. RapiGest detergent was obtained from Waters. All polyacrylamide gels, protein ladder, PVDF membranes, and other gel running supplies were obtained from Invitrogen. Cell culture reagents were acquired from Invitrogen. Purified band 3 protein was kindly supplied by the Low group (Purdue University), and purified Cdk and Cdc6 proteins were generously provided by the Hall group (Purdue University). Plasmid DNA was transfected with MegaTran (OriGene) as described by the manufacturer. BI 2536 inhibitor was purchased from Symansis. The synthetic peptide library used for label-free quantitation was generously provided by Dr. Randy Arnold from Indiana University.

Synthesis of pIMAGO—Solution of 200 μl of polyamidoamine dendrimer generation 4 (provided as 10% (w/v) in methanol) was dried in a microcentrifuge tube and resolubilized in 2 ml of DMSO. Biotin (7 mg) was added to the solution to functionalize dendrimer with biotin molecules. Ten mg of hydroxybenzotriazole and 12 μl of 1,3-diisopropylcarbodiimide were added to activate the carboxylic acid group of the biotin for coupling with ~30% of the amine groups on the dendrimer. The reaction was stirred overnight at room temperature. The reaction solution was dialyzed against water using SnakeSkin® pleated dialysis tubing (3,500 molecular weight cutoff, 22-mm dry diameter) and concentrated using a 3,000 molecular weight cutoff

[1] The abbreviations used are: pIMAGO, phosphorimaging; Cdc6, cell division cycle 6; Cdk, cyclin-dependant kinase; CIAP, calf intestine alkaline phosphatase; HRP, horseradish peroxidase; IP, immunoprecipitation/immunoprecipitated; Plk1, Polo-like kinase 1; Syk, spleen tyrosine kinase; KD, kinase dead.

centrifugal filter unit (Millipore) to remove unreacted chemicals and concentrate the modified dendrimer. The solution was further mixed with 1.5 ml of 250 mM MES buffer (pH 5.5), 2 mg of 2-carboxyethylphosphonic acid, 8 mg of *N*-hydroxysuccinimide dissolved in 100 μl of water, and 80 mg of 1-ethyl-3-(3-dimethylaminopropyl) carbodiimide hydrochloride and stirred overnight at room temperature to functionalize the dendrimer with phosphonic acid. The reaction solution was dialyzed again to remove unreacted chemicals and stored at 4 °C. One-third of the reagent solution was concentrated to 1 ml, and 10 μl of titanium oxychloride stock in 30% HCl was added. The mixture was incubated for 1 h with agitation at room temperature to chelate titanium ions with phosphonic acid groups on the dendrimer. The final solution was again dialyzed to remove any unbound titanium and stored at 4 °C.

Dot-blotting of Standard Proteins and pIMAGO-based Detection—Membrane for dot-blot assays was soaked in methanol, and different amounts of standard proteins were each spotted in 0.5 μl of total volume. The membrane was allowed to dry, followed by blocking with 10 ml of SuperBlock T20 blocking buffer containing 1% BSA for 1 h. The membrane was then rinsed with water and incubated for 1 h with 5 μl of the pIMAGO reagent (0.4 mM in 0.01% HCl, pH 5) in 10 ml of 500 mM glycolic acid, 1% TFA solution, pH 0.75. The dot-blot was washed four times with the 500 mM glycolic acid, 1% TFA solution and three times with 1× TBST, 5 min each wash. For detection, the membrane was incubated with 1:5000 dilution of avidin-peroxidase in 1× TBST (Tris-buffered saline containing 0.1% Nonidet P-40, pH 7.5) containing 1% BSA for 45 min while rocking. The membrane was lastly washed four times with 1× TBST (5 min each) and detected with ECL detection solution.

Cell Culture, Anti-Tyr(P) IP, and Protein Dephosphorylation—HeLa cells were grown to confluency in Dulbecco's modified Eagle's medium supplemented with fetal bovine serum, 1% sodium pyruvate, and 0.5% streptomycin/penicillin. The cells (6×10^7) were trypsinized, collected, and lysed in 1 ml of lysis solution (50 mM Tris-HCl, pH 7.5, 150 mM NaCl, 5 mM EDTA, 1% Nonidet P-40, 1 mM sodium orthovanadate, 1× protease inhibitor mixture, 1× phosphatase inhibitor mixture, and 10 mM sodium fluoride) for 20 min on ice. The cell debris was cleared at 16,100 × *g* for 10 min, and supernatant containing soluble proteins was collected. The concentration of the cell lysate was determined using the bicinchoninic protein assay.

Two sets of 1 mg cell lysate were incubated with 40 μl of anti-phosphotyrosine antibody (clone PT66) conjugated to agarose beads for 2 h at 4 °C. The beads were then washed with the lysis buffer, and the bound proteins were eluted with 100 mM triethanolamine. The elutions were then dried and resuspended in 25 mM of Tris-Cl buffer, pH 7.5. For dephosphorylation assay, one-half of each elution was incubated with 10 units of calf intestine alkaline phosphatase (CIAP) in 1× CIAP buffer (50 mM Tris-Cl, 100 mM NaCl, 10 mM $MgCl_2$, 1 mM dithiothreitol) for 30 min at 37 °C. To stop the enzyme activity, the samples were boiled for 5 min in 1× SDS sample buffer.

In Vitro Phosphatase and Kinase Assays—For *in vitro* phosphatase assay, 200 ng of ovalbumin and β-casein were incubated with 2 units of CIAP in 1× CIAP buffer (50 mM Tris-Cl, 100 mM NaCl, 10 mM $MgCl_2$, 1 mM dithiothreitol) for 30 min at 37 °C. Equal percentages of the reaction solution were taken out at designated times and boiled for 5 min in 1× SDS sample buffer. The samples were run on an SDS gel, transferred onto a PVDF membrane, and blotted with pIMAGO as described above. After exposure, the membrane was stripped using the stripping buffer (62.5 mM Tris-Cl, 2% SDS, 0.7% β-mercaptoethanol, pH 6.7) for 30 min at 65 °C and stained with Coomassie Blue stain (0.1% Brilliant Blue in the solution containing 10% acetic acid, 45% methanol, 45% water) to detect the overall protein signal.

For *in vitro* kinase assays, 200 ng each of band3 or Cdc6 were incubated with 500 μM of ATP and 2 mM of $MnCl_2$ (for Syk) or $MgCl_2$ (for Cdk) in the presence of their respective kinase (200 ng). An equal amount of each reaction solution was taken out at designated times and boiled for 5 min in 1× SDS sample buffer. The samples were run on an SDS gel, transferred onto a PVDF membrane, and blotted with pIMAGO as described before. After detection of the Syk-band3 reaction with pIMAGO, the membrane was stripped by incubation with the stripping buffer (62.5 mM Tris-Cl, 2% SDS, 0.7% β-mercaptoethanol, pH 6.7) for 30 min at 65 °C. The membrane was then blocked and incubated overnight at 4 °C with anti-phosphotyrosine antibody (4G10 clone). After washing and incubation with secondary anti-mouse antibody for 45 min, the membrane was exposed again to detect anti-Tyr(P) signal. Finally, both membranes were stripped using the stripping buffer and stained with Coomassie blue stain to detect overall protein signal.

Detection of Endogenous Phosphorylation of Plk1-interacting Proteins—HEK 293T cells were transfected with FLAG-Plk1 wild-type or K82M mutant (kinase dead mutant). After transfection for 24 h, the cells were enriched at mitosis by nocodazole (100 ng/ml) treatment for 12 h. For cells transfected with FLAG-Plk1-K82M, BI 2536 (Plk1 inhibitor, 100 nM) was added for the last 8 h before harvest. Both sets of cells (5×10^7 cells) were lysed in 500 μl of lysis solution (50 mM Tris-HCl, pH 7.5, 150 mM NaCl, 1% Nonidet P-40, 1 mM sodium orthovanadate, 1× phosphatase inhibitor mixture (Sigma), 1× protease inhibitor mixture, 10 mM sodium fluoride) for 20 min on ice. The cell debris was cleared at 16,100 × *g* for 10 min, and supernatant containing soluble proteins was collected, resulting in 4 mg of protein amount in each sample. At this stage, a small volume of both lysates was stored at −20 °C for the Western blotting. The remaining lysates were precleared with 20 μl of protein A/G-agarose beads for 20 min at 4 °C, and the supernatant was collected. For Plk1 IP, the samples were incubated for 2 h with 40 μl of anti-FLAG beads at 4 °C. Finally, the supernatant was discarded, the beads were washed twice with the lysis solution for 10 min each, and 25% of the beads were used to elute the bound proteins by boiling in 2× SDS solution containing 40 mM DTT for 5 min at 95 °C. The resulting samples (including the set-aside lysates) were run on an SDS gel (40 μg of lysates or one-half of IP elutions), transferred onto a PVDF membrane, and blotted with pIMAGO as described before. After the detection with pIMAGO, the membrane was stripped by incubation with the stripping buffer (62.5 mM Tris-Cl, 2% SDS, 0.7% β-mercaptoethanol, pH 6.7) for 30 min at 65 °C. The membrane was then blocked and incubated overnight at 4 °C with anti-phosphothreonine antibody. After washing and incubation with secondary anti-rabbit antibody for 45 min, the membrane was exposed again to detect anti-Thr(P) signal. Finally, the membrane was stripped again using the stripping buffer and blotted for 1 h with anti-FLAG antibody at room temperature. The FLAG-tagged Plk1 signal was detected after incubation with secondary anti-rabbit antibody for 45 min.

For the detection of pIMAGO signal using fluorescence, IRDye 680 fluorophore-tagged streptavidin was used instead of avidin-HRP. In this case, the incubation was carried out using same conditions as before, except the detection was done out using Li-Cor Odyssey infrared imager, set at the wavelength channel of 700 nm and the intensity setting of 0.5.

Mass Spectrometry-based Phosphoproteomic Analysis—The remaining 75% of the beads left after anti-FLAG immunoprecipitation (from ~3 mg starting protein amount) were used for the phosphoproteomics experiment. The bound proteins were eluted off beads, denatured, and reduced by incubating the beads in 50 mM trimethylammonium bicarbonate containing 0.2% RapiGest and 10 mM dithiothreitol for 5 min at 95 °C. After collecting the supernatant (eluted proteins), the samples were cooled to room temperature and incubated with 30 mM iodoacetamide for 1 h in the dark to alkylate the cysteines. The pH was adjusted to 8.0, and the samples were di-

gested with 1 μg trypsin for 14 h at 37 °C. Following digestion, RapiGest was removed by decreasing pH to below 3.0 with 1 N hydrochloric acid, incubating the samples at 37 °C for 40 min, centrifuging it down for 10 min at 16,100 $\times$ *g*, and collecting the supernatant. The resulting digested peptides were then enriched by PolyMAC method to isolate phosphopeptides, as described before (25).

The eluted phosphopeptides were dried and redissolved in 8 μl of 0.5% formic acid. At this stage, 100 fmol of 220 peptide library was added to each sample as internal standard to enable label-free quantitation and injected into an Eksigent two-dimensional Ultra nanoflow HPLC system. The reverse phase C18 was performed using an in-house C18 capillary column packed with 5 μm C18 Magic beads resin (Michrom; 75-μm inner diameter and 30 cm of bed length). The mobile phase buffer consisted of 0.1% HCOOH in ultra-pure water with the eluting buffer of 100% CH_3CN run over a shallow linear gradient over 60 min with a flow rate of 0.3 μl/min. The electrospray ionization emitter tip was generated on the prepacked column with a laser puller (model P-2000; Sutter Instrument Co.). The Eksigent Ultra HPLC system was coupled online with a high resolution hybrid linear ion trap Orbitrap mass spectrometer (LTQ-Orbitrap Velos; Thermo Fisher). The mass spectrometer was operated in the data-dependent mode in which a full-scan MS (from *m/z* 300–2000 with the resolution of 30,000) was followed by 20 MS/MS scans of the most abundant ions. Ions with charge state of +1 were excluded. The mass exclusion time was 90 s. The LTQ-Orbitrap raw files were searched directly against the *Homo sapiens* database with no redundant entries (91,464 entries; human International Protein Index v.3.87) using a combination of SEQUEST algorithm and MASCOT on Proteome Discoverer (version 1.3; Thermo Fisher). Peptide precursor mass tolerance was set at 10 ppm, and MS/MS tolerance was set at 0.8 Da. Search criteria included a static modification of cysteine residues of +57.0214 Da and a variable modifications of +15.9949 Da to include potential oxidation of methionines, and a modification of +79.996 Da on serine, threonine, or tyrosine for the identification of phosphorylation. Searches were performed with full tryptic digestion and allowed a maximum of two missed cleavages on the peptides analyzed from the sequence database. False discovery rates were set below 1% for each analysis. Proteome Discoverer generates a reverse "decoy" database from the same protein database, and any peptides passing the initial filtering parameters that were derived from this decoy database are defined as false positive identification. The minimum cross-correlation factor filter was then readjusted for each individual charge state separately to optimally meet the predetermined target false discovery rate of 1% based on the number of random false-positive matches from the reversed "decoy" database. Thus, each data set had its own passing parameters. The most likely phosphorylation site localization from collision-induced dissociation mass spectra was determined by PhosphoRS algorithm within the Proteome Discoverer 1.3 software.

Phosphopeptides identified by Mascot and SEQUEST with a statistical significant threshold were quantified by in-house software (manuscript in preparation). MASIC (27) integrated in the software uses the *m/z* of the selected peptides to construct extracted ion chromatograms with default settings. Windows for extracted ion chromatogram construction were 5 ppm. The relative intensity value of each peptide was calculated by the peak area of each individual extracted ion chromatogram normalized to the total chromatogram intensity of 220 equally spiked-in peptides mixture. Two identical peptides that have a significant intensity ratio, which is more than 3 or less than 0.33, between two samples are considered to have different phosphorylation level. At least two biological replicates were performed for the analysis.

The data associated with this manuscript, specifically the MS/MS spectra and the raw MS files, may be downloaded from ProteomeCommons.org Tranche, https://proteomecommons.org/tranche/, using the following hash code: KSeBmSNefSWKnYB66DFXtpMT9So8CtRf5xZ0U5PQl6C4AtYsS1eKbdsqXaskdYMb2IcECd/x05fo4A6a44OJQMkZsmsAAAAAAAAEIQ==.

RESULTS

Design of pIMAGO Strategy for Phosphoprotein Detection on Membrane—The design of pIMAGO is based on a soluble nanopolymer, *i.e.*, dendrimer, with hyperbranched surface groups for derivatization. In addition to high solubility under aqueous conditions, the advantages of using soluble nanopolymer include high structural and chemical homogeneity, compact spherical shape, and controlled surface functionalities (28). The homogeneous and hyperbranched nature of the functionalized nanopolymer exhibited high reactivity and superior specificity toward phosphorylated molecules (25).

The general pIMAGO scheme for phosphorylation detection on membrane is shown in Fig. 1. The dendrimer polyamidoamine G4 was functionalized with 15–20 titanium(IV) ions for strong and selective binding to the phosphate groups and with 25–30 biotin groups per pIMAGO molecule to achieve sensitive chemiluminescence-based detection using avidin-linked HRP (Fig. 1*A*). After proteins are transferred onto a membrane, the detection procedure closely resembles a standard Western blotting protocol, where the membrane is blocked with BSA in a detergent-containing buffer, followed by incubation with the pIMAGO reagent for 1 h in place of a primary antibody and the use of avidin-HRP instead of a secondary antibody (Fig. 1*B*). Therefore, with the pIMAGO molecule acting as a sequence-independent anti-phosphoprotein antibody, the overall procedure is common and can be easily adapted by any life science laboratory. Furthermore, the blotting is completely compatible with any subsequent antibody-based detection because of the ability to efficiently strip the pIMAGO-based signal off the membrane after detection or to detect both signals simultaneously in a fluorescence-based multiplexed procedure.

Selectivity and Sensitivity of pIMAGO-based Detection—To initially test the ability of pIMAGO to selectively detect phosphorylated proteins, we performed dot-blotting analysis of two commercially available standard phosphorylated (α-casein and ovalbumin) and two nonphosphorylated (α-lactalbumin and β-lactoglobulin) proteins. After spotting 100 ng of each protein, the membrane was blocked and incubated with pIMAGO regent. After the avidin-HRP step, the blot was incubated with HRP substrate and exposed onto a film. As shown in Fig. 2*A*, only the two phosphoproteins were detected on a dot-blot, indicating good selectivity of pIMAGO toward phosphate detection. As expected, the signal from α-casein has appeared much stronger than from ovalbumin, likely because of the relatively larger number of phosphorylated residues in the former.

To further test the selectivity and sensitivity of the pIMAGO technology, we spotted five standard proteins in different

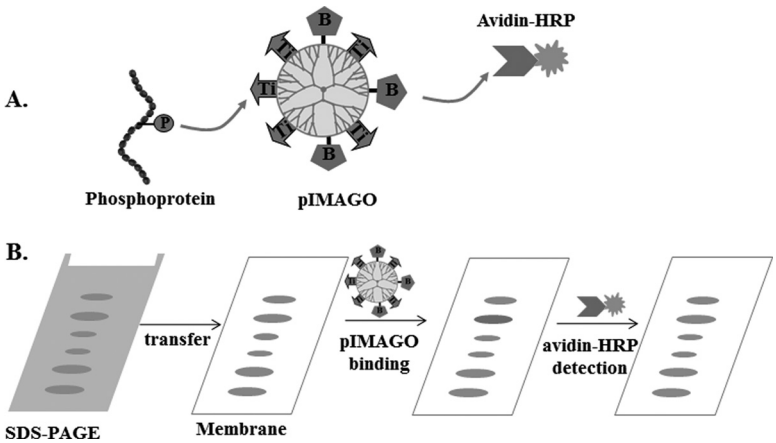

FIG. 1. **A schematic representation of the pIMAGO reagent.** *A*, a soluble nanopolymer (dendrimer) is functionalized with multiple titanium ions for selective binding to the phosphoproteins and with biotin groups for sequential detection by avidin-linked HRP. *B*, experimental workflow for pIMAGO-based phosphoprotein detection in a Western blotting format. After SDS-PAGE of the protein mixture and transfer onto a PVDF membrane, the blot is briefly incubated with the pIMAGO reagent, which selectively binds to phosphosites. HRP-linked avidin is then added to the membrane, exclusively attaching to the biotin groups of pIMAGO. Finally, a chemiluminescent HRP substrate is added, and the membrane is developed for detection.

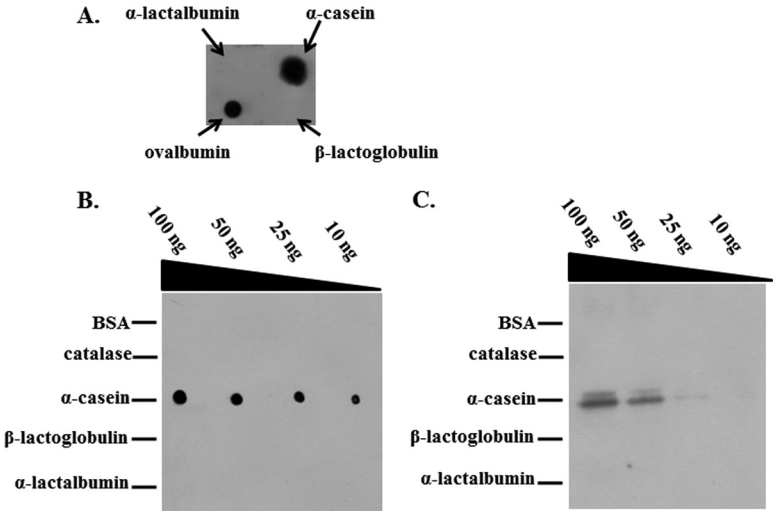

FIG. 2. **pIMAGO-based detection of phosphoproteins.** *A*, a dot-blotting experiment, where two phosphoproteins (α-casein and ovalbumin) and two nonphosphoproteins (α-lactalbumin and β-lactoglobulin) were spotted on a PVDF membrane and detected using pIMAGO procedure. *B*, a dot-blotting experiment, where phosphorylated α-casein and four nonphosphoproteins (α-lactalbumin, β-lactoglobulin, BSA, and catalase) were spotted at different amounts on PVDF membranes and detected using pIMAGO procedure. *C*, pIMAGO-based detection of different concentrations of the five-protein mixture separated by SDS-PAGE and transferred onto a PVDF membrane. The mixture included phosphorylated α-casein and four nonphosphoproteins (α-lactalbumin, β-lactoglobulin, BSA, and catalase).

amounts, ranging from 10 to 100 ng, for a pIMAGO-based dot-blot analysis. The proteins included phosphorylated α-casein and four unphosphorylated proteins (BSA, catalase, α-lactalbumin, and β-lactoglobulin). The results, shown in Fig. 2*B*, demonstrate good selectivity and sensitivity of the blotting reagent, allowing detection of only phosphorylated α-casein, even below 10 ng levels.

We have further explored the ability of pIMAGO to selectively detect phosphoproteins in a Western blotting format by mixing together the same five proteins at different concentrations, separating the mixture on a gel, and transferring onto a PVDF membrane. As shown in Fig. 2*C*, pIMAGO-based blotting again was able to detect only the phosphoprotein with good sensitivity, although the background was slightly higher than the dot blotting because of the presence of SDS on the membrane after gel transfer, which led to somewhat lower sensitivity. Taken together, these data suggest that pIMAGO could be a valuable tool for the detection of phosphorylation after SDS-PAGE separation and transfer.

Additional testing of the blotting selectivity was carried out using a more complex sample, a protein mixture isolated by anti-phosphotyrosine antibody-based immunoprecipitation

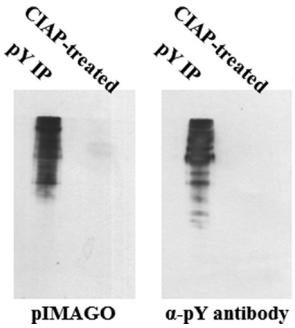

FIG. 3. **pIMAGO-based detection of a complex mixture of phosphoproteins.** Cell lysate was used to immunoprecipitate (*IP*) phosphotyrosine-containing proteins (*pY*). One-half of each IP elution was dephosphorylated by general CIAP. Finally, the control and CIAP-treated samples were split in two, separated by SDS-PAGE, transferred onto a membrane, and detected independently using pIMAGO or anti-phosphotyrosine antibody.

(anti-Tyr(P) IP). With 1 mg of HeLa lysate as the starting material, the resulting protein complex was split equally in halves. One sample was dephosphorylated with a general CIAP. Two samples were run alongside on the SDS-PAGE gel, transferred onto a membrane, and blotted independently using either pIMAGO or anti-phosphotyrosine antibody. The results demonstrated a significant decrease in signal from the phosphatase-treated samples in both cases, indicating that pIMAGO is highly specific for phosphoproteins in a complex sample (Fig. 3). Interestingly, proteins show a different pattern when detected by pIMAGO compared with the general anti-Tyr(P) antibody approach: a number of new bands were detected using the pIMAGO method. The new bands are likely due to the ability of pIMAGO to detect not only phosphotyrosine proteins, which is the case for the anti-Tyr(P) antibody, but also phosphoserine and phosphothreonine residues. It is also possible that some of the new protein bands are phosphotyrosine proteins that cannot be detected by this particular clone of anti-Tyr(P) antibody. The experiment revealed that pIMAGO can be used to detect any phosphoprotein without the bias that antibodies may have.

Applications of pIMAGO for in Vitro Kinase and Phosphatase Assays—Because pIMAGO has demonstrated its ability to detect any phosphorylation without bias, it would be particularly useful for the detection of changes in phosphorylation during *in vitro* kinase and phosphatase assays. These procedures, although routine, can provide invaluable knowledge about the kinase-substrate or phosphatase-substrate relations and can be used to identify or validate new interesting substrates. Typically, such an approach requires either preliminary knowledge of the phosphorylation sites, in the case of antibody-based detection; the use of artificial substrates, which could provide misleading information; or handling of the highly hazardous radioactive materials, in the case of ^{32}P-based reactions. To address the limitations and high cost of the antibodies and the safety concerns of the radioactive assays, we attempted to examine whether pIMAGO is capable of detecting changes in phosphorylation during *in vitro* kinase or phosphatase assays.

We first tested the capability of pIMAGO in detecting time-dependent dephosphorylation of standard proteins during an *in vitro* phosphatase assay. Phosphoproteins, ovalbumin, and β-casein were utilized as substrates for a general CIAP. The dephosphorylation reaction was carried out for the designated time points, and the assay mix was run on an SDS gel and transferred onto a membrane. The previously described pIMAGO procedure was then carried out to detect the level of phosphorylation. As shown in Fig. 4*A*, a strong decrease in phosphorylation was detected for both proteins, with ovalbumin losing signal much faster, most likely because of somewhat differential substrate specificity of CIAP.

We further carried out *in vitro* kinase assays with a purified tyrosine kinase, human Syk, and a serine/threonine kinase, yeast Cdk1, along with their known substrates, band3 (29, 30) and Cdc6 (31), respectively. Each kinase reaction was carried out for the designated time points, and each assay mix was run on an SDS gel and transferred. For the Syk-band3 kinase assay, the membrane was also blotted with a general anti-Tyr(P) antibody after pIMAGO. On the other hand, because no successful general anti-serine/threonine antibody is available, Cdk1-Cdc6 kinase reaction was blotted only with pIMAGO. As is demonstrated in Fig. 4 (*B* and *C*), both kinase reactions resulted in increased levels of phosphorylation, as was detected by pIMAGO and confirmed by anti-Tyr(P) antibody blotting. Coomassie staining was also carried out for the assays to ensure equal loading.

Our experiments demonstrate that pIMAGO has the potential to complement the often unnecessary or ineffective and costly phosphospecific antibodies and the hazardous radioactive labeling approach for routine kinase activity assays. This technology has the potential for high sensitivity because there are multiple biotin detection groups per molecule, thus amplifying the detection signal. The technique is particularly appealing to research groups that work with new or uncharacterized kinases and their substrates, whose phosphorylation profiles are unknown. Instead of designing experiments to map potential phosphorylation sites of their substrates to make new phospho-specific antibodies, the pIMAGO reagent can be readily used for a majority of initial kinase assays for any substrate.

Detection of Endogenous Phosphorylation of Plk1-interacting Proteins—In addition to the use of pIMAGO in the Western blot format for detection of *in vitro* phosphorylation, the technology also offers great potential for examining *in vivo* or endogenous phosphorylation. To validate this idea, we have selected serine/threonine kinase Plk1 and its interacting proteins as our model system. Plk1 is a member of an important Polo-like kinase family and is a well known key regulator in many cell cycle events. As a serine/threonine kinase, Plk1 activity in mitosis is critical for proper regulation of mitotic entry, cytokinesis, bipolar spindle formation, and sister chro-

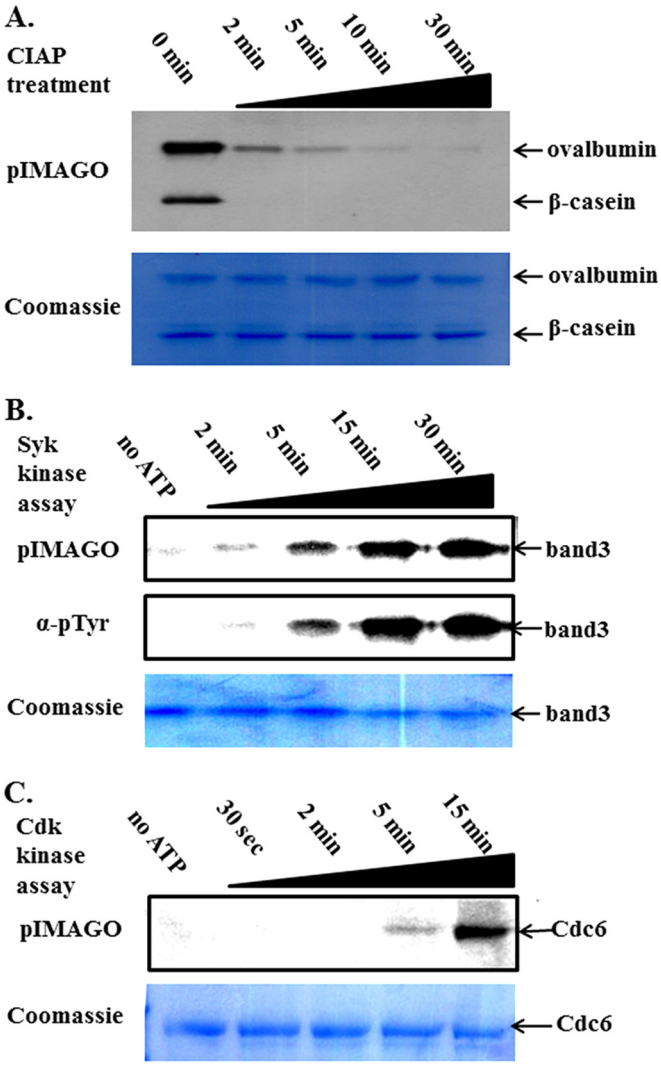

FIG. 4. ***In vitro* phosphatase and kinase assays using pIMAGO.** *A*, two phosphoproteins (*β*-casein and ovalbumin) were treated with CIAP for the indicated times. Each assay time point was run on the SDS gel, transferred onto a membrane, and blotted by pIMAGO. *B*, *in vitro* kinase assay of Syk tyrosine kinase and its substrate band3 was carried out for the indicated times. Phosphorylation change on the substrate was monitored by pIMAGO; the membrane was then stripped and reprobed with anti-phosphotyrosine antibody. *C*, *in vitro* kinase assay of Cdk serine/threonine kinase and its substrate Cdc6 was carried out for the indicated times. Phosphorylation change on the substrate was detected by pIMAGO. In all cases, Coomassie stain was performed to ensure equal loading.

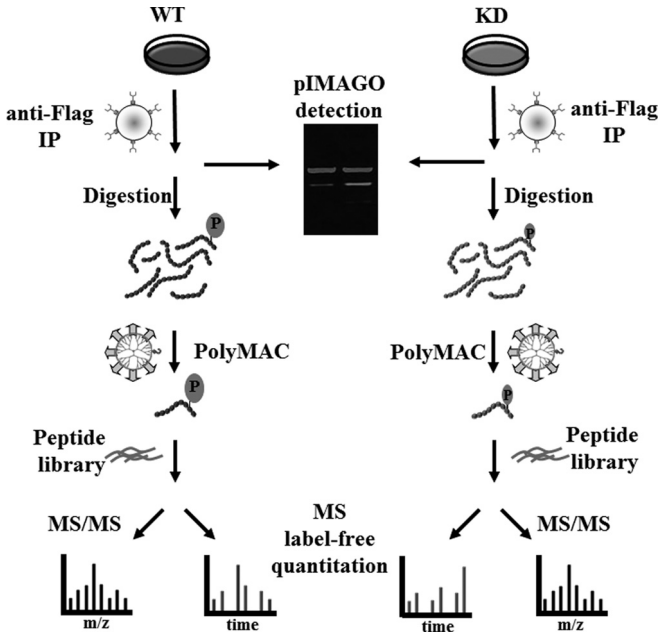

FIG. 5. **Experimental workflow of pIMAGO detection and phosphoproteomic analysis of Plk1-interacting proteins.** FLAG-Plk1 WT or FLAG-Plk1-KD (kinase dead mutant) were transfected into HEK 293T cells and arrested in mitosis, and the cells were lysed. The interacting protein partners for Plk1 were separately pulled down by anti-FLAG antibody conjugated with beads. At this stage, 25% of each sample were eluted, run on SDS-PAGE, transferred onto a membrane, and detected by pIMAGO. The remaining 75% were trypsin-digested, and phosphopeptides were enriched by PolyMAC method. Prior to mass spectrometry analysis, a peptide library consisting of 220 unique peptides was spiked into each sample for label-free quantitation.

matid separation (32–34). In addition, it has also been suggested that Plk1 plays an important role in the network of DNA damage checkpoint (35, 36). Taking this into account, it is not surprising that numerous recent studies have demonstrated a strong correlation between mammalian Plk1 expression and cancer (33, 37). Its overexpression has been well documented in many carcinomas, including non-small cell lung cancer, ovarian cancer, gastric cancer, melanoma, and others (33, 38). Therefore, selective inhibition of Plk1 activity may provide an important complementary tool in cancer therapy. Plk1 has been involved in multiple signaling pathways, and its tumorigenic features are tightly related to its modulated phosphorylation events and interacting partners (38). To better understand the role of Plk1 in normal cells and cancer progression, it is of critical importance to examine the protein signaling in the Plk1-dependent network.

To assess the phosphorylation levels of Plk1-interacting proteins, HEK 293T cells were transfected with FLAG-tagged Plk1 and arrested in mitosis where Plk1 is most active. As a comparison, the cells were also transfected to express a kinase dead (KD) mutant of Plk1, and BI 2536, a specific Plk1 inhibitor (39, 40), was incubated with these cells. Both sets of samples were immunoprecipitated using anti-FLAG antibody, run on an SDS-PAGE, and detected via pIMAGO. Simultaneously, to validate the pIMAGO imaging results and identify the Plk1-interacting proteins obtained using pIMAGO detection system, we used 75% of the immunoprecipitated samples to run a quantitative phosphoproteomics experiment using mass spectrometry (general workflow is demonstrated in Fig. 5). As expected, both sets of lysates and IP samples showed high levels of phosphorylation (Fig. 6*A*). The phosphorylation signal of the wild-type Plk1 lysate was slightly higher compared with

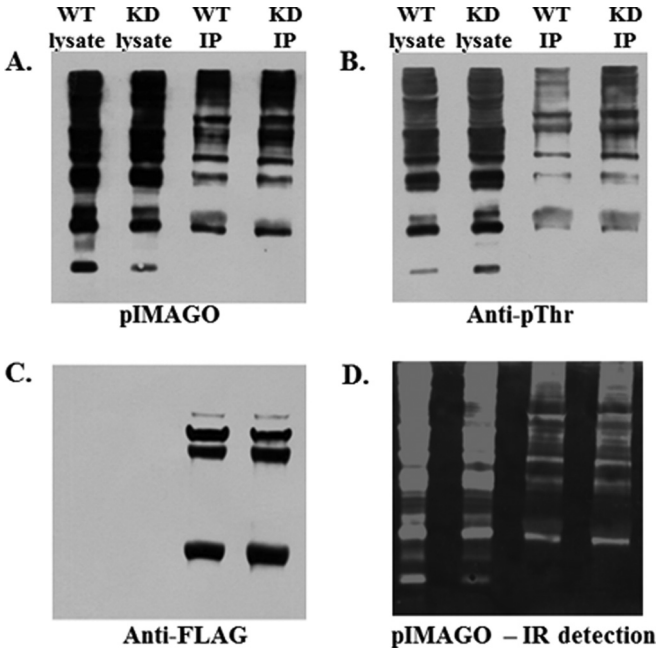

FIG. 6. **pIMAGO-based detection of phosphorylation from lysates and IP samples of wild-type Plk1 and its KD mutant.** HEK 293T lysates were used to IP FLAG-tagged WT- or KD-Plk1. *A–C*, the samples were separated by SDS-PAGE, transferred onto a membrane, and detected using pIMAGO (A), anti-phosphothreonine (*Anti-pThr*) antibody (*B*), or anti-FLAG antibody (*C*). The membrane was stripped before each subsequent detection. *D*, the same experiment as in *A* was carried out, but the pIMAGO signal was detected using IRDye 680 fluorophore conjugated to streptavidin instead of HRP-based chemiluminescence.

the Plk1-KD lysate, likely because of increased activity of the Plk1 kinase. Interestingly, IP of Plk1-KD mutant clearly exhibited a higher level of phosphorylation in the interacting proteins compared with wild-type kinase. As a comparison, the membrane was also blotted using an anti-Thr(P) antibody, which showed a similar phosphorylation pattern, although only of threonine sites (Fig. 6*B*). An anti-FLAG Western blotting was further carried out as a loading control (Fig. 6*C*). These data suggest that the phosphorylation levels of Plk1-interacting proteins are higher in the kinase dead mutant of the kinase. The data confirmed the perception that kinase-substrate interactions are typically weak and transient. Once substrates are phosphorylated, the interactions are even weaker, leading to the dissociation of substrates from the kinase. On the other hand, KD mutant has stronger binding affinity to its substrates because the post-activity release does not occur, which can then be captured by IP. These results demonstrate that pIMAGO technique can provide an overall profile of phosphorylation status in kinase complexes.

In parallel with the pIMAGO detection experiment, the immunoprecipitated interacting protein partners for Plk1 were eluted off the beads and trypsin-digested, and phosphopeptides were enriched by the PolyMAC method. Prior to mass spectrometry analysis, a synthetic peptide library consisting of 220 unique peptides was spiked into each sample for label-free quantitation. Here, each sample peptide was normalized based on the overall signal of the library. Via this approach, the use of such a large peptide library enabled a more accurate label-free quantitation by allowing normalization of the sample's signal to that of the library across a wide LC retention time range (manuscript on the label-free approach in preparation).

Using this phosphoproteomics procedure, we were able to identify a total of 490 unique phosphopeptides covering 272 proteins (qualitative data are available in supplemental Table S1 for Plk1 identifications and supplemental Table S2 for library identifications). Of these, 182 phosphorylated proteins (with 266 unique phosphopeptides) were denoted as the potential Plk1 substrates or interaction partners dependent on Plk1 activity, because they were present at significantly higher levels in the Plk1-KD immunoprecipitated sample compared with wild-type samples, where they were often not detectable (quantitative results are available in supplemental Table S3). Interestingly, the majority of these peptides contained a consensus sequence for Cdk1 ((pS/pT)P) (41), consistent with the reports that recognition of Plk1 substrates requires a priming kinase to generate a docking site for Plk1 recruitment (42). Among the candidates, some were reported previously as putative Plk1 targets, such as Claspin (43, 44), Foxhead box protein M1 (45), 53BP1 (46), Sororin (47), Nek9 (48), and Wee1 (49). As expected, the phosphopeptides identified from the kinase dead Plk1 IP sample did not contain the Plk1 phosphorylation sites, but rather some potential priming sites by Cdk1 or other kinases. More importantly, we have also identified several previously undescribed potential Plk1 targets, such as CENPA, Nup153, and FoxO1, thus implicating that Plk1 may function in kinetochore specification, regulation of nucleus-cytoplasm translocation, and determination of stem cell fate.

The quantitative proteomic data by mass spectrometry was further compared with fluorescence-based pIMAGO detection. In the experiment, we replaced avidin-HRP with IRDye 680 fluorophore-labeled streptavidin. Generally, there are certain advantages to using a fluorophore as a detection system. Compared with dynamic chemiluminescence-based system, fluorescent detection allows for measurements in a static state, without the need for enzymatic substrates, danger of overexposing, or the possibility of exhausting the substrates or enzyme activity. Additionally, direct detection typically offers a shorter procedure, up to 10-fold greater linear dynamic range and better quantitative capability (an example of pIMAGO-based detection and IRDye-based quantitation of standard phosphoproteins on membrane is demonstrated in supplemental Fig. S1). In this case, the same experiment as above was carried out, and the phospho-bound pIMAGO signal was detected using a Li-Cor Odyssey infrared imager. The resulting phosphorylation pattern (Fig. 6*D*) was similar to the chemiluminescence signal in Fig. 6*A*, thereby demonstrat-

ing potential applications of pIMAGO for studies that prefer fluorescence-based detection. Furthermore, fluorescence-based pIMAGO detection allowed us to quantify an average of 40% increase in the level of phosphorylation in the Plk1-KD-bound proteins from the immunoprecipitated sample, which is consistent with the measurement by label-free mass spectrometry analyses (supplemental Fig. S2).

DISCUSSION

The ubiquity and importance of protein phosphorylation has become increasingly better understood and appreciated over the past decades. It is estimated that close to 50% of all proteins in the human genome are phosphorylated during their lifetime on over 100,000 sites (50). With such astonishing numbers, it is no wonder that protein phosphorylation is perhaps the most widespread post-translational modification known. Its involvement in practically all aspects of cell biology has been demonstrated through numerous examinations. Although the genes encode the basic biological functions of proteins, post-translational modifications, in particular phosphorylation, are responsible for real time regulation of protein functions and structure, usually in response to stimuli. Therefore, the fundamental importance of phosphorylation cannot be overestimated. As a result, effective detection of protein phosphorylation has long been a major objective in many life science research laboratories.

To date, detection of phosphorylation has continuously been under development, and many of the currently available methods suffer from certain drawbacks, such as the need for extensive prior knowledge and high cost, as in the case of antibodies, hazardous environment during ^{32}P labeling, or low specificity and sensitivity of non-antibody-based staining. We attempt to address these concerns by developing a novel universal phosphorylation detection technology based on Ti(IV)-functionalized soluble nanopolymer, pIMAGO. The nanosize nature of the water-soluble polymer offers multiple advantages for manipulating molecular interactions. Its dendritic structure allows multifunctionalization, offering enhanced selectivity, stronger binding to target, and greater sensitivity because of signal amplification. Furthermore, the choice of Ti(IV) ion as the chelating metal is the direct result of numerous published reports (including our own) about titanium, demonstrating superior selectivity toward phosphate groups compared with other metal ions (22, 23, 25, 51). Thus, pIMAGO is expected to display superior selectivity to other universal stains based on the metal selection alone.

We demonstrate in this study that pIMAGO can detect phosphoproteins immobilized on a membrane in simple or complex mixtures with high selectivity. We have applied it for *in vitro* kinase and phosphatase assays, producing comparable results as the antibodies. However, in contrast to antibodies, pIMAGO can be used for the detection of phosphorylation on any site for any protein without the amino acid sequence bias. Although phospho-site specific antibodies are still the optimal choice of detecting the phosphorylation level of a particular site on the protein of interest, this piece of information is not necessary or available for many types of research projects. Most often, the first step in molecular signaling studies is to identify whether a protein of interest demonstrates any change in phosphorylation under specific biological conditions, a positive identification of which can then be subsequently followed by an in-depth examination of modified sites. In these experiments, as well as in most *in vitro* assays to test kinase/phosphatase activity, a more general approach for detection of phosphorylation, such as pIMAGO, would be much more valuable and cost-effective. Note that other phospho-containing molecules such as phospholipids may interfere with analysis of phosphoproteins, and therefore a preseparation such as gel electrophoresis might be needed. On the other hand, pIMAGO is not limited to the analysis of phosphoproteins. It is conceivable that pIMAGO will be effective for the detection of phospho-containing molecules such as phospholipids.

We further demonstrated the utility of pIMAGO-based on-membrane detection for analysis of endogenous phosphorylation. For this purpose, we have selected Plk1-interacting proteins, a biological system important for regulation of a number of mitotic and DNA damage events and having a direct link to certain cancers. Immunoprecipitation of the kinase dead mutant of Plk1 (Plk1-KD) during mitosis with subsequent detection with pIMAGO exhibited a 40% increase in the overall level of phosphorylation within its interacting proteins, as compared with wild-type Plk1. We reason that this increase in phosphorylation is due to potential Plk1 substrates still being bound to Plk1-KD during IP, because they could not be released from the inactive kinase. A label-free quantitative phosphoproteomics experiment confirmed the pIMAGO observation. The MS data have resulted in the identification of 182 unique phosphoproteins that were bound in a considerably higher proportion to the Plk1-KD than to wild-type Plk1. Of these, we were able to identify a significant amount of known interacting partners and substrates, including Claspin, Foxhead box protein M1, Nek9, 53BP1, Sororin, and Wee1. Among them, there are multiple proteins such as CENPA, Nup153, and FoxO1 proteins that are likely new candidates for Plk1 phosphorylation.

FoxO1 belongs to the forkhead family of transcriptional factors (52) and has been previously implicated in maintaining embryonic stem cell pluripotency, regulating cell death, DNA damage repair, and tumor suppression (53). Plk1 is reported to phosphorylate FoxM1, another member from this forkhead transcription factor family, to regulate mitotic gene expressions (45). The functional significance of Plk1-FoxO1 interaction would be interesting to investigate further.

CENPA, a histone H3 variant, specifies the assembly of kinetochore on centromeric region (54). CENPA recruits the constitutive centromere-associated network, a 14-component protein complex, to form the inter kinetochore, which

provides the structural base for the functional mitotic kinetochore (55). Although Plk1 is implicated in kinetochore function (56), whether Plk1 is involved in kinetochore specification is largely unknown.

Nup153 belongs to the nuclear pore complex protein family, which is involved in nuclear pore assembly (57). Nuclear pores are large protein complexes that cross the nuclear envelope, and biological molecules such as proteins and RNAs are transported through the nuclear pore between the cytoplasm and the nucleus (58). Identification of Nup153 as potential Plk1 substrate indicates a previously undescribed role of Plk1 in regulating this cytoplasm-nucleus translocation.

Although Plk1 is implicated to function in kinetochore specification (56), regulation of nucleus-cytoplasm translocation (59), and stem cell pluripotency (60), the molecular mechanisms of these events remain unclear. Therefore, further characterization of these potential Plk1 substrates will provide insight to biological functions of Plk1 in these pathways.

CONCLUSIONS

A novel application using soluble nanopolymer-based pIMAGO technology was presented for the detection of phosphorylated proteins in the Western blotting format. The procedure is specific, sensitive, and easy to perform. The unique capabilities of pIMAGO toward unbiased detection of phosphoproteins hold great promise for a wide variety of applications *in vitro* and *in vivo*. The technique may not be applicable to hyperphosphorylated proteins in which only a specific single site changes its phosphorylation status, thus not significantly affecting overall phosphorylation level of the protein. We are currently exploring the possibility of quantitative measurement of phosphorylation changes, including phosphorylation stoichiometry. The novel technique, however, is highly attractive to applications in which a good quality phospho-specific antibody is not available. The ability to facilitate the finding of new kinase and phosphatase substrates, screen kinase inhibitors, or profile changes in endogenous levels of phosphorylation without site microenvironment prejudice or safety concerns will be tremendously valuable for many research groups.

* This work was supported in part by National Science Foundation Career Award CHE-0645020, National Institutes of Health Grant 1R01GM088317, and funds from the National Institute of Food and Agriculture.

[S] This article contains supplemental material.

‡ To whom correspondence should be addressed. E-mail: watao@purdue.edu.

REFERENCES

1. Hunter, T. (2000) Signaling: 2000 and beyond. *Cell* **100,** 113–127
2. Blume-Jensen, P., and Hunter, T. (2001) Oncogenic kinase signalling. *Nature* **411,** 355–365
3. Pandey, A., Podtelejnikov, A. V., Blagoev, B., Bustelo, X. R., Mann, M., and Lodish, H. F. (2000) Analysis of receptor signaling pathways by mass spectrometry: Identification of vav-2 as a substrate of the epidermal and platelet-derived growth factor receptors. *Proc. Natl. Acad. Sci. U.S.A.* **97,** 179–184
4. Guy, G. R., Philip, R., and Tan, Y. H. (1994) Analysis of cellular phosphoproteins by two-dimensional gel electrophoresis: Applications for cell signaling in normal and cancer cells. *Electrophoresis* **15,** 417–440
5. Hu, V. W., and Heikka, D. S. (2000) Radiolabeling revisited: Metabolic labeling with ^{35}S-methionine inhibits cell cycle progression, proliferation, and survival. *FASEB J.* **14,** 448–454
6. Hu, V. W., Heikka, D. S., Dieffenbach, P. B., and Ha, L. (2001) Metabolic radiolabeling: Experimental tool or Trojan horse? ^{35}S-Methionine induces DNA fragmentation and p53-dependent ROS production. *FASEB J.* **15,** 1562–1568
7. Aebersold, R., and Goodlett, D. R. (2001) Mass spectrometry in proteomics. *Chem. Rev.* **101,** 269–295
8. Mann, M., and Jensen, O. N. (2003) Proteomic analysis of post-translational modifications. *Nat. Biotechnol.* **21,** 255–261
9. Steen, H., Jebanathirajah, J. A., Rush, J., Morrice, N., and Kirschner, M. W. (2006) Phosphorylation analysis by mass spectrometry: Myths, facts, and the consequences for qualitative and quantitative measurements. *Mol. Cell. Proteomics* **5,** 172–181
10. Green, M. R., Pastewka, J. V., and Peacock, A. C. (1973) Differential staining of phosphoproteins on polyacrylamide gels with a cationic carbocyanine dye. *Anal. Biochem.* **56,** 43–51
11. Goldberg, H. A., and Warner, K. J. (1997) The staining of acidic proteins on polyacrylamide gels: Enhanced sensitivity and stability of "Stains-all" staining in combination with silver nitrate. *Anal. Biochem.* **251,** 227–233
12. Steinberg, T. H., Agnew, B. J., Gee, K. R., Leung, W. Y., Goodman, T., Schulenberg, B., Hendrickson, J., Beechem, J. M., Haugland, R. P., and Patton, W. F. (2003) Global quantitative phosphoprotein analysis using Multiplexed Proteomics technology. *Proteomics* **3,** 1128–1144
13. Martin, K., Steinberg, T. H., Cooley, L. A., Gee, K. R., Beechem, J. M., and Patton, W. F. (2003) Quantitative analysis of protein phosphorylation status and protein kinase activity on microarrays using a novel fluorescent phosphorylation sensor dye. *Proteomics* **3,** 1244–1255
14. Stasyk, T., Morandell, S., Bakry, R., Feuerstein, I., Huck, C. W., Stecher, G., Bonn, G. K., and Huber, L. A. (2005) Quantitative detection of phosphoproteins by combination of two-dimensional difference gel electrophoresis and phosphospecific fluorescent staining. *Electrophoresis* **26,** 2850–2854
15. Liu, J., Cai, Y., Wang, J., Zhou, Q., Yang, B., Lu, Z., Jiao, L., Zhang, D., Sui, S., Jiang, Y., Ying, W., and Qian, X. (2007) Phosphoproteome profile of human liver Chang's cell based on 2-DE with fluorescence staining and MALDI-TOF/TOF-MS. *Electrophoresis* **28,** 4348–4358
16. Orsatti, L., Forte, E., Tomei, L., Caterino, M., Pessi, A., and Talamo, F. (2009) 2-D Difference in gel electrophoresis combined with Pro-Q Diamond staining: A successful approach for the identification of kinase/phosphatase targets. *Electrophoresis* **30,** 2469–2476
17. Goodman, T., Schulenberg, B., Steinberg, T. H., and Patton, W. F. (2004) Detection of phosphoproteins on electroblot membranes using a small-molecule organic fluorophore. *Electrophoresis* **25,** 2533–2538
18. Kinoshita, E., Kinoshita-Kikuta, E., Takiyama, K., and Koike, T. (2006) Phosphate-binding tag, a new tool to visualize phosphorylated proteins. *Mol. Cell. Proteomics* **5,** 749–757
19. Barbieri, C. M., and Stock, A. M. (2008) Universally applicable methods for monitoring response regulator aspartate phosphorylation both *in vitro* and *in vivo* using Phos-tag-based reagents. *Anal. Biochem.* **376,** 73–82
20. Kinoshita, E., and Kinoshita-Kikuta, E. (2011) Improved Phos-tag SDS-PAGE under neutral pH conditions for advanced protein phosphorylation profiling. *Proteomics* **11,** 319–323
21. Kinoshita, E., Kinoshita-Kikuta, E., and Koike, T. (2009) Separation and detection of large phosphoproteins using Phos-tag SDS-PAGE. *Nat. Protoc.* **4,** 1513–1521
22. Pinkse, M. W., Uitto, P. M., Hilhorst, M. J., Ooms, B., and Heck, A. J. (2004) Selective isolation at the femtomole level of phosphopeptides from proteolytic digests using 2D-NanoLC-ESI-MS/MS and titanium oxide precolumns. *Anal. Chem.* **76,** 3935–3943
23. Larsen, M. R., Thingholm, T. E., Jensen, O. N., Roepstorff, P., and Jørgensen, T. J. (2005) Highly selective enrichment of phosphorylated peptides from peptide mixtures using titanium dioxide microcolumns. *Mol. Cell. Proteomics* **4,** 873–886
24. Jensen, S. S., and Larsen, M. R. (2007) Evaluation of the impact of some

experimental procedures on different phosphopeptide enrichment techniques. *Rapid Commun. Mass Spectrom.* **21,** 3635–3645
25. Iliuk, A. B., Martin, V. A., Alicie, B. M., Geahlen, R. L., and Tao, W. A. (2010) In-depth analyses of kinase-dependent tyrosine phosphoproteomes based on metal ion functionalized soluble nanopolymers. *Mol. Cell. Proteomics* **9,** 2162–2172
26. Iliuk, A., Martinez, J. S., Hall, M. C., and Tao, W. A. (2011) Phosphorylation assay based on multifunctionalized soluble nanopolymer. *Anal. Chem.* **83,** 2767–2774
27. Monroe, M. E., Shaw, J. L., Daly, D. S., Adkins, J. N., and Smith, R. D. (2008) MASIC: A software program for fast quantitation and flexible visualization of chromatographic profiles from detected LC-MS(/MS) features. *Comput. Biol. Chem.* **32,** 215–217
28. Boas, U., and Heegaard, P. M. (2004) Dendrimers in drug research. *Chem. Soc. Rev.* **33,** 43–63
29. Harrison, M. L., Isaacson, C. C., Burg, D. L., Geahlen, R. L., and Low, P. S. (1994) Phosphorylation of human erythrocyte band 3 by endogenous p72 Syk. *J. Biol. Chem.* **269,** 955–959
30. Brunati, A. M., Bordin, L., Clari, G., James, P., Quadroni, M., Baritono, E., Pinna, L. A., and Donella-Deana, A. (2000) Sequential phosphorylation of protein band 3 by Syk and Lyn tyrosine kinases in intact human erythrocytes: Identification of primary and secondary phosphorylation sites. *Blood* **96,** 1550–1557
31. Elsasser, S., Lou, F., Wang, B., Campbell, J. L., and Jong, A. (1996) Interaction between yeast Cdc6 protein and B-type cyclin/Cdc28 kinases. *Mol. Biol. Cell* **7,** 1723–1735
32. Nigg, E. A. (1998) Polo-like kinases: Positive regulators of cell division from start to finish. *Curr. Opin. Cell Biol.* **10,** 776–783
33. Strebhardt, K. (2010) Multifaceted polo-like kinases: Drug targets and antitargets for cancer therapy. *Nat. Rev. Drug Discov.* **9,** 643–660
34. van Vugt, M. A., and Medema, R. H. (2005) Getting in and out of mitosis with Polo-like kinase-1. *Oncogene* **24,** 2844–2859
35. Syljuåsen, R. G., Jensen, S., Bartek, J., and Lukas, J. (2006) Adaptation to the ionizing radiation-induced G2 checkpoint occurs in human cells and depends on checkpoint kinase 1 and Polo-like kinase 1 kinases. *Cancer Res.* **66,** 10253–10257
36. Studach, L., Wang, W. H., Weber, G., Tang, J., Hullinger, R. L., Malbrue, R., Liu, X., and Andrisani, O. (2010) Polo-like kinase 1 activated by the hepatitis B virus X protein attenuates both the DNA damage checkpoint and DNA repair resulting in partial polyploidy. *J. Biol. Chem.* **285,** 30282–30293
37. Murugan, R. N., Park, J. E., Kim, E. H., Shin, S. Y., Cheong, C., Lee, K. S., and Bang, J. K. (2011) Plk1-targeted small molecule inhibitors: Molecular basis for their potency and specificity. *Mol. Cells* **32,** 209–220
38. Liu, X. S., Song, B., and Liu, X. (2010) The substrates of Plk1, beyond the functions in mitosis. *Protein Cell* **1,** 999–1010
39. Lénárt, P., Petronczki, M., Steegmaier, M., Di Fiore, B., Lipp, J. J., Hoffmann, M., Rettig, W. J., Kraut, N., and Peters, J. M. (2007) The small-molecule inhibitor BI 2536 reveals novel insights into mitotic roles of polo-like kinase 1. *Curr. Biol.* **17,** 304–315
40. Steegmaier, M., Hoffmann, M., Baum, A., Lénárt, P., Petronczki, M., Krssák, M., Gürtler, U., Garin-Chesa, P., Lieb, S., Quant, J., Grauert, M., Adolf, G. R., Kraut, N., Peters, J. M., and Rettig, W. J. (2007) BI 2536, a potent and selective inhibitor of polo-like kinase 1, inhibits tumor growth in vivo. *Curr. Biol.* **17,** 316–322
41. Alexander, J., Lim, D., Joughin, B. A., Hegemann, B., Hutchins, J. R., Ehrenberger, T., Ivins, F., Sessa, F., Hudecz, O., Nigg, E. A., Fry, A. M., Musacchio, A., Stukenberg, P. T., Mechtler, K., Peters, J. M., Smerdon, S. J., and Yaffe, M. B. (2011) Spatial exclusivity combined with positive and negative selection of phosphorylation motifs is the basis for context-dependent mitotic signaling. *Sci Signal.* **4,** ra42
42. Barr, F. A., Silljé, H. H., and Nigg, E. A. (2004) Polo-like kinases and the orchestration of cell division. *Nat. Rev. Mol. Cell Biol.* **5,** 429–440
43. Mamely, I., van Vugt, M. A., Smits, V. A., Semple, J. I., Lemmens, B., Perrakis, A., Medema, R. H., and Freire, R. (2006) Polo-like kinase-1 controls proteasome-dependent degradation of Claspin during checkpoint recovery. *Curr. Biol.* **16,** 1950–1955
44. Yoo, H. Y., Kumagai, A., Shevchenko, A., and Dunphy, W. G. (2004) Adaptation of a DNA replication checkpoint response depends upon inactivation of Claspin by the Polo-like kinase. *Cell* **117,** 575–588
45. Fu, Z., Malureanu, L., Huang, J., Wang, W., Li, H., van Deursen, J. M., Tindall, D. J., and Chen, J. (2008) Plk1-dependent phosphorylation of FoxM1 regulates a transcriptional programme required for mitotic progression. *Nat. Cell Biol.* **10,** 1076–1082
46. van Vugt, M. A., Gardino, A. K., Linding, R., Ostheimer, G. J., Reinhardt, H. C., Ong, S. E., Tan, C. S., Miao, H., Keezer, S. M., Li, J., Pawson, T., Lewis, T. A., Carr, S. A., Smerdon, S. J., Brummelkamp, T. R., and Yaffe, M. B. (2010) A mitotic phosphorylation feedback network connects Cdk1, Plk1, 53BP1, and Chk2 to inactivate the G_2/M DNA damage checkpoint. *PLoS Biol.* **8,** e1000287
47. Zhang, N., Panigrahi, A. K., Mao, Q., and Pati, D. (2011) Interaction of sororin protein with Polo-like kinase 1 mediates resolution of chromosomal arm cohesion. *J. Biol. Chem.* **286,** 41826–41837
48. Bertran, M. T., Sdelci, S., Regué, L., Avruch, J., Caelles, C., and Roig, J. (2011) Nek9 is a Plk1-activated kinase that controls early centrosome separation through Nek6/7 and Eg5. *EMBO J.* **30,** 2634–2647
49. Watanabe, N., Arai, H., Iwasaki, J., Shiina, M., Ogata, K., Hunter, T., and Osada, H. (2005) Cyclin-dependent kinase (CDK) phosphorylation destabilizes somatic Wee1 via multiple pathways. *Proc. Natl. Acad. Sci. U.S.A.* **102,** 11663–11668
50. Bergström Lind, S., Molin, M., Savitski, M. M., Emilsson, L., Aström, J., Hedberg, L., Adams, C., Nielsen, M. L., Engström, A., Elfineh, L., Andersson, E., Zubarev, R. A., and Pettersson, U. (2008) Immunoaffinity enrichments followed by mass spectrometric detection for studying global protein tyrosine phosphorylation. *J. Proteome Res.* **7,** 2897–2910
51. Zhou, H., Ye, M., Dong, J., Han, G., Jiang, X., Wu, R., and Zou, H. (2008) Specific phosphopeptide enrichment with immobilized titanium ion affinity chromatography adsorbent for phosphoproteome analysis. *J. Proteome Res.* **7,** 3957–3967
52. Galili, N., Davis, R. J., Fredericks, W. J., Mukhopadhyay, S., Rauscher, F. J., 3rd, Emanuel, B. S., Rovera, G., and Barr, F. G. (1993) Fusion of a fork head domain gene to PAX3 in the solid tumour alveolar rhabdomyosarcoma. *Nat. Genet.* **5,** 230–235
53. Kousteni, S. (2011) FoxO1: A molecule for all seasons. *J. Bone Miner. Res.* **26,** 912–917
54. Prasad, P., and Ekwall, K. (2011) New insights into how chromatin remodellers direct CENP-A to centromeres. *EMBO J.* **30,** 1875–1876
55. McAinsh, A. D., and Meraldi, P. (2011) The CCAN complex: Linking centromere specification to control of kinetochore-microtubule dynamics. *Semin. Cell Dev. Biol.* **22,** 946–952
56. Cheeseman, I. M., and Desai, A. (2008) Molecular architecture of the kinetochore-microtubule interface. *Nat. Rev. Mol. Cell Biol.* **9,** 33–46
57. Ball, J. R., and Ullman, K. S. (2005) Versatility at the nuclear pore complex: Lessons learned from the nucleoporin Nup153. *Chromosoma* **114,** 319–330
58. Hoelz, A., Debler, E. W., and Blobel, G. (2011) The structure of the nuclear pore complex. *Annu. Rev. Biochem.* **80,** 613–643
59. Toyoshima-Morimoto, F., Taniguchi, E., and Nishida, E. (2002) Plk1 promotes nuclear translocation of human Cdc25C during prophase. *EMBO Rep.* **3,** 341–348
60. Wang, H., Ouyang, Y., Somers, W. G., Chia, W., and Lu, B. (2007) Polo inhibits progenitor self-renewal and regulates Numb asymmetry by phosphorylating Pon. *Nature* **449,** 96–100